Current Research on the ARO-Positron Emission Tomography

Meei-Ling Jan*, Hsing-Ching Liang, Shin-Wen Huang, Chuen-Shing Shyu
Jiy-Shan Tang, Hong-Chih Liu, Cheng-Chih Pei, Ching-Kai Yeh

Physics Division, Institute of Nuclear Energy Research, Taiwan, ROC.

ABSTRACT

We are presently constructing "AROPET", a rotating PET scanner for imaging small animals. The design of the system has flexible geometry, using four detectors. Each detector is made of a position-sensitive PMTs (Hamamatsu R3941) coupled with 18x16 small individual BGO scintillator crystals of dimension 2.6x2.6x25mm^3. Animals can be imaged in two modes. One is similar to a gamma camera in which the detectors are stationary and a 2-D planar projection imaging is obtained. This mode is used for initial characterization of the bio-distribution of tracers. In the other mode the detectors are rotated through 90°,and the diameter can be adjusted between 22cm~40cm. This mode resembles a conventional 3-D PET scan using a partial detector ring. Thirty-one tomographic images can be obtained after rebinning and reconstruction. The field of view is 51.3 mm (transaxial) by 45.6mm (axial). The spatial resolution of the planar projection mode, and the results of the planar image of a phantom and the dynamical images of the bio-distribution of F18-FDG in a mouse are discussed.

Keywords: Positron Emission Tomography, PET, planar projection imaging

1. INTRODUCTION

Animal models of human diseases are widely used in basic biomedical research to elucidate disease mechanism and to develop and test new treatments. Positron Emission Tomography (PET), an ideal, powerful tool in modern biology, allows the distribution of radiolabeled tracers of biological interest to be measured quantitatively and dynamically in living animals[1,2]. The ability to make repeated measurements on the same animal is unique to PET and confers an important advantage over traditional autoradiographic and tissue counting assays. In the basic research using experimental animals, research are interesting in the study of physiological process and the chemistry in living subjects. The animal PET experiments play an important role in basic research for bio-functions and in application studies such as the development of new drugs. However, PET systems developed for human used do not process sufficient spatial resolution and sensitivity to accurately quantify changing organ radioactivity in small animals(mice, rats). Therefore, a number of groups have thought to overcome this limitation by developing high performance PET systems specifically for imaging small animals[3-8]. In this report, we describe an imaging system, ARO-PET (Animal ROtational PET), developed in our laboratory for the purpose of imaging mice and rats with two imaging modes, 2-D planar projection imaging and 3-D rotational tomography imaging. The scanner of the ARO-PET based on BGO crystals coupled to position-sensitive photomultiplier tube (PSPMT). The geometry of the scanner is flexible and allows adjusting the center-detector distance according to the sensitivity requirement and the size of the object being scanned.

2. SYSTEM DESCRIPTION

A. Design Features

The design of the system has flexible geometry, using two pairs of detectors. The four detectors are mounted on a rotating plate which can be rotated by 90° during a scan by a stepper motor. The center-detector distance can be adjusted from 11cm~20cm. The configuration of the ARO-PET is shown in Figure 1.

The scanner has two emission imaging modes: 2-D planar and 3-D rotational (figure 2a, 2b). The 2-D planar mode produces planar projection images by using only one pair of detectors. From the detectors, signals in coincidence are readout and identified to two crystals by lookup tables. The planar imaging is performed by back-projecting lines of response joining theses crystals. This mode will be valuable for measuring the distribution of radiotracer in an animal body as a function of time. The field-of-view (FOV) of the planar image is 51.3mm x 45.6mm.

* Correspondences: Meei-Ling Jan Email: mljan@iner.gov.tw ; TEL: 886-3-4711400 ext.7403; FAX: 886-3-4711408

In *Input/Output and Imaging Technologies II*, Yung-Sheng Liu, Thomas S. Huang, Editors,
Proceedings of SPIE Vol. 4080 (2000) • 0277-786X/00/$15.00

The rotational mode allows the four detectors to rotate around an object and obtains 3-D tomographic images. In this mode, the 3-D data mode will be rebinned to thirty-one sinograms, and be reconstructed by using 2-D Filtered-Backprojection algorithm[9]. This mode has the transaxial FOV 51.3 mm and the axial FOV 45.6mm.

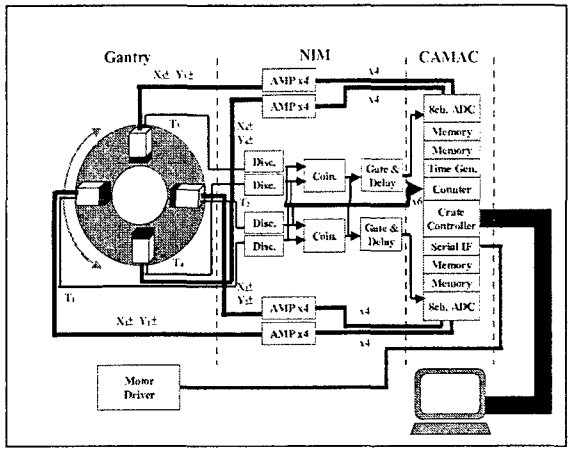

Figure 1: System schematic

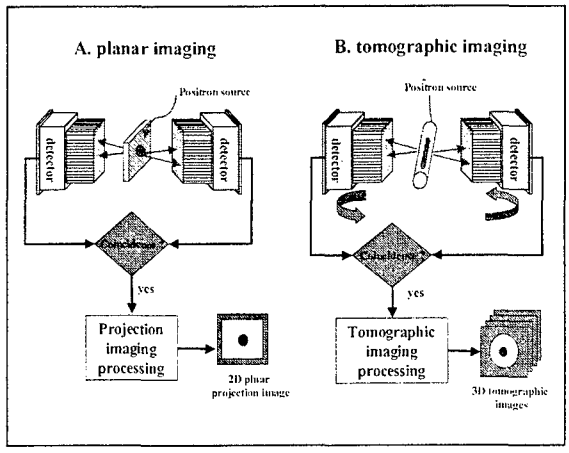

Figure 2: The ARO-PET has two imaging modes, planar imaging and rotaional imaging. For rotational mode, all four detectors are used, although in this figure only two detectors are drawn.

B. Detectors

One detector block consists of 18x16 small individual BGO scintillator crystals of dimension 2.6x2.6x25mm^3. All crystals are optically isolated by being wrapped with PTFE tape(figure 3). The crystal matrix is coupled to a PSPMT (Hamamatsu R3941). These detectors are mounted diagonally opposite to each other for detection pairs of the 511keV gamma rays. Since the two gamma rays produced from positron-electron annihilation are simultaneously emitted 180° apart, a logic AND module for timing coincidence is used to define the line of emission.

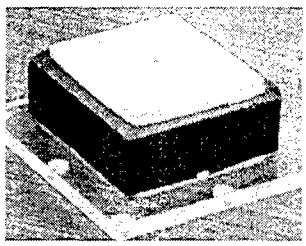

Figure 3: 18x16 crystal matrix

C. Data acquisition Electronics

The four signals, two for the x-direction and two for y-direction, from a PS-PMT are fed into a FERA ADC LeCroy 4300B for determining the x and y positions (x=(x1-x2)/(x1+x2) , y=(y1-y2)/(y1+y2)) and for pulse height (energy) analysis. The resulting four 11-bit data words are transferred by ECL-FERA bus to a FERA memory (LeCroy 4302 model) for temporally restored. After the FERA 4302 (32K words capacity) being full, all the data are transferred to a PC hard disk by CAMAC Dataway[10] via a PCI plug-in board KS2915 for advanced data processing. While a FERA memory is transferred data to PC, the other FERA memory replaces it to record the data from the ADC. Using two FERA memories to work in turn can minimize the dead time due to readout of the memory by CAMAC transfer. A timing signal from the last dynode of the PS-PMT is input a leading edge discriminator for suppressing low level noise, and then to a logic gate NIM (Nuclear Instrument Module) module LeCroy 365AL to determine whether the two detectors are truly in coincidence corresponding to a real positron annihilation. During a measurement, the LeCroy 365AL checks the coincidence condition with a coincident timing window 20ns and the ADC values represented the positions as well as the energy information are stored in list mode.

D. Data Acquisition and Control Software

The data acquisition in 3D mode is performed by a PC, which also controls the stepper motors. After setting the scanned time and the number of rotating angle by an operator, the program starts to control the rotating plate and when the

plate has reached to its appropriate angle position, the program turns on the FERA ADCs and FERA memories[11]. During data acquisition, one of the 4302 memories is disabled (via CAMAC commands) and the ADC is enabled. Once the active memory asserts the LAM (Look-At-Me)[10], the ADC is halted, the second memory is enabled, and then the ADC is cleared and enabled. While the data is being collected by the enabled memory, the data in the other memory is moved using block transfer to the PC. The process is repeated when the enabled memory asserts a LAM. Till the acquisition time has been achieved then the CAMAC modules are inhibit, and the data in the memory is transferred to the PC. After that the rotating plate rotates to the next angle, and the ADCs and the memories start again. The whole process is repeated until the detectors being rotated by 90°.

3. RESULTS

A. signals and effective counting rates Improvement

Position sensitive PMTs we used have a large Position dependent gain inhomogeneity, which leads to large position dependent variations in signal intensity. There are two problems of these detectors: (1) while the PSPMT's high voltage is not high enough (above the operation voltage 1000V already), parts of the crystals' responses are deficient. This is because some of the intensities of the signals can not exceed the discriminator's threshold, although the threshold level of discriminator has been adjusted as low as possible. This causes less the effective counting rate and sensitivity. (2) The other problem is that when the PSPMT's high voltage increases, the crystals' responses increase also, however some of them increase too many to be overflowed. Since the FERA 4300B ADC has its highest current limitation, the ADC value shows overflow while the intensity of signal from the detector exceeds the limitation. If one of the four signals from the same detector occurs overflow, this event will be not valuable for position and energy calculation. Therefore, the overflow of signal will cause the effective counting rate decreased. This can be seen in the table 1 and the figure 4. From the view of the energy spectrum, it shows in the figure 5 left, most of the overflowed signals should have the energy around the 511keV. So the loss of the overflowed signals will cause the coincident events with the primary energy to be lost. To avoid these problems, we adjusted the detectors' high voltage to 1250V, and used the home made attenuators with different factors for different detectors for reducing the signal intensity as well as the signal overflowed rate.

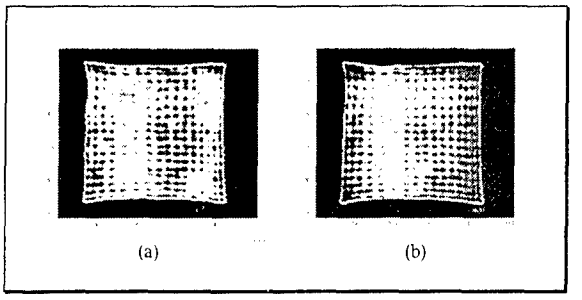

Figure 4: (a)before, and (b) after signal improvement. It shows in panel (b), the inhomogeneity of the crystal's response has been improved.

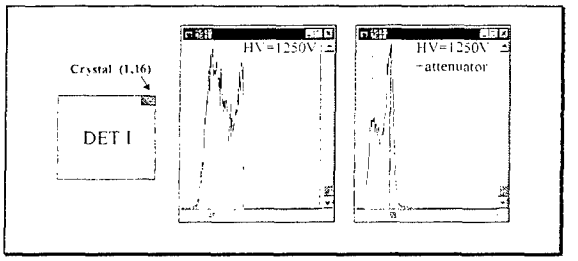

Figure 5: Energy spectrums of a crystal of the I detector. Left: most of the primary events are overflowed and can mot be recorded. Right: More the primary events are collected by adding the attenuator to avoid the overflow of the signals.

B. 2-D Planar Imaging

We used a phantom to obtain the 2-D planar imaging. All compartments of the phantom were filled with the F18-FDG solution. Figure 6 shows the planar projection image of this phantom. The scanned time was 5 minutes. Center-detector distance was 11cm. It is shown in figure 6, the upper part of the phantom image has higher activity, this is because the diameters of the upper part of the phantom are bigger. This is designed for the convenience of injecting in and drawing out the FDG solution from the phantom. Except the solution entrance and exit parts of phantom, the other parts are with the diameter of 2mm.

The spatial resolution of the planar imaging of the ARO-PET was measured using a phantom with seven bars filled with F18-FDG. These bars are 4mm, 4mm, 3mm, 5mm, 5mm apart. The diameters of these bars are 2mm. Figure 7 shows the spatial resolution of the planar imaging of the ARO-PET system is 3mm or less.

First animal studies were performed also with the F18-FDG. The anaesthetized mouse was placed on the imaging bed, and it was injected with 0.5mCi F18-FDG. The center-Detector distance was 11cm. Scanning was started 10 minutes after injection for 60 minutes. The animal was viewed in face up with the nose at the top, the tail at the bottom. The lower half of the animal was in the field-of-view. Figure 8 shows the planar projection images of this experiment. The planar images of the 20mins, 40mins, 60mins after scanning being begun are shown. The brighter objects at the bottom of these images are the bladders. It shows that at the first 20mins only little of F18-FDG was accumulated at the bladder, but in the period of last 20mins there was the most F18-FDG being drained into the bladder, so the image of the bladder was the brightest. This experiment shows that the positron-emitting tracer can be dynamically followed with this device.

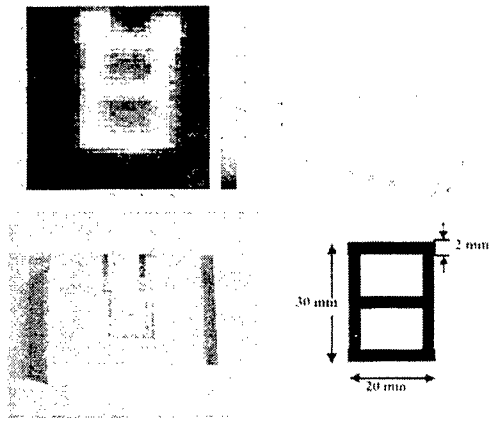

Figure 6: Planar image of a "日" phantom. The phantom was filled with F18-FDG.

4. PERSPECTIVES AND DISCUSSION

The ARO-PET has been built over the last year in the Institute of Nuclear Energy Research. During fabrication it was realize the PSPMTs we got have defects in there. So the position response of the detectors were unsymmetry. After repairing the PSPMTs by the HAMAMATSU, we rebuilt the detectors and increased the crystal matrix to 18 x 16 to enlarge the FOV(51.3mm x 45.6mm). The signals from the detectors and effective counting rate are also improved. It is shown in this paper, the initial results obtained from the ARO-PET are encouraging. The planar imaging mode with spatial resolution less than 3mm can carry out a wide variety of studies with this device. For example, the dynamic planar projection image could be applied to time-activity curve measurements, and presents novel opportunities for modeling the transport of new radiopharmaceuticals and changes in organ function due to genetic or other manipulations. Besides, several experiments[11-13] showed the positron-based planar projection imaging technique can be applied to nonmedical applications, for example, to trace the uptake and transport of positron-emitting tracer in plants to observe the damage and recovery functions of plants *in vivo* .

We are currently working on measuring the rotating tomograpghic images. After further testing, we shall apply the tomographic mode of the ARO-PET system for phantoms and animal studies. Parameters such as the spatial and timing resolution, efficiency, and count-rate performance will be evaluated also.

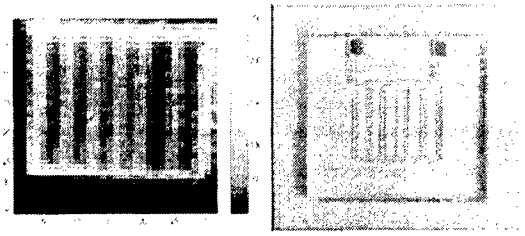

Figure 7: Planar image of a seven-bar phantom. The phantom was filled with F18-FDG. The seven bars are 4mm, 4mm, 3mm, 3mm, 5mm, 5mm apart.

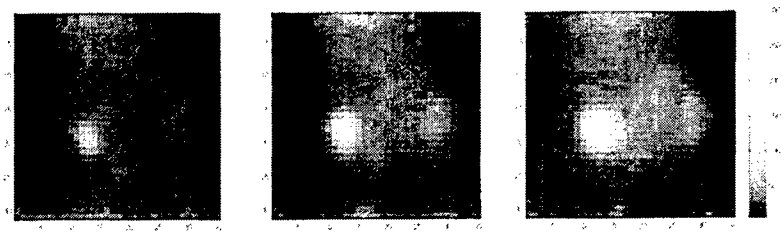

Figure 8: Planar images of a live mouse's lower half part. From left to right: sum image from 10~30mins, 30~50mins, 50~70mins after injection are shown. The bright objects are the bladder.

High Voltage	1150V	1175V	1200V	1250V
Effective Counting Rate (counts/sec)	2421	4632	6748	5388
Overflowed Rate(%)	1.7	1.9	4.1	22.8

Table 1: The effective counting rates and the overflowed rates of ADC values are varied with high voltage supply.

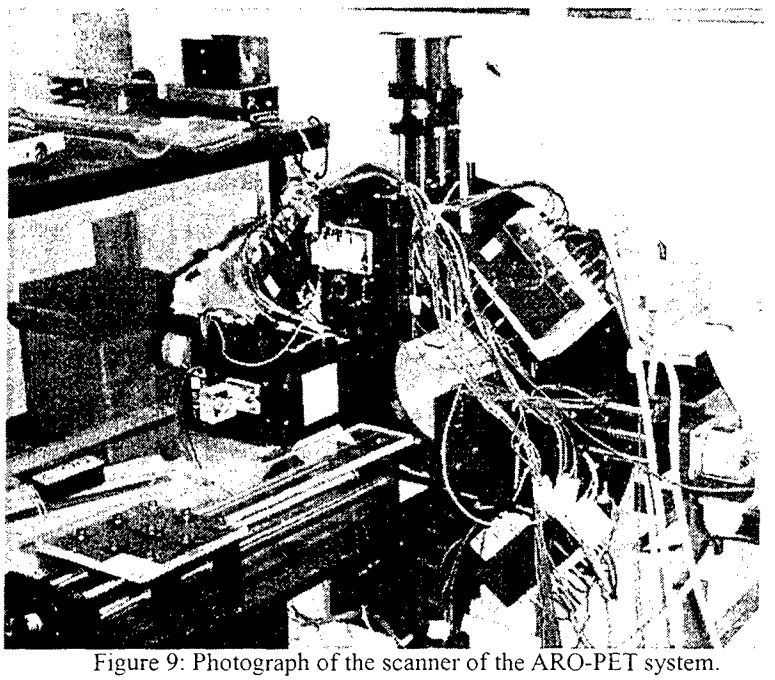

Figure 9: Photograph of the scanner of the ARO-PET system.

5. ACKNOWLEDGMENTS

The authors would like to thank the Isotope Applications Division of the Institute of Nuclear Energy Research, Taiwan, for supporting in producing the F18-FDG, and in preparing the anesthetized animals.

6. REFERENCE

1. M.P. Sandler, *et al.*, "Diagnostic Nuclear Medicine", Volume I, 3rd Edition, William & Wilkins, USA, 1996.
2. R.D. Hichwa, "Are animal scanners really necessary for PET?", *J. Nucl. Med.*, **35**, 1396-1397, 1994.
3. A.A. Lammertsma, "PET scanners for small animals", *J. Nucl. Med.*, **36**, 2391-2391, 1995.
4. S.R.Cherry, *et al.*, "MicroPET:a high resolution PET scanner for imaging small animals", *IEEE Trans. Nucl. Sci.*, **44**, 1161-1166, 1997.
5. M. Watanabe, *et al.*, "A high resolution PET for animal studies", *IEEE Trans. Imag.* **11**, 577-580, 1992.
6. R. Lecomte, *et al.*, "Initial results from the Sherbrooke Avalanche Photodiode Positron Tomograph", *IEEE Trans. Nucl. Sci*, **43**, 1952-1957, 1996.
7. S.Weber, *et al.*, "Evaluation of the TierPET system", *IEEE Trans. Nucl. Sci.*, **46**, 1177-1183,1999.
8. S.Siegel, *et al.*, "Initial results from a PET/Planar small animal imaging system", *IEEE Trans. Nucl. Sci.*, **46**, 571-575,1999.
9. R.A. Brooks, *et al.*, "Principles of computer assisted tomography (CAT) in radiographic and radioisotopic imaging", *Phys. Med. Biol.*, **21**, 689-732, 1976.

10. "An introduction to CAMAC", Lecroy 1994 Research Instrumentation Catalog.
11. T.K.Lewellen, *et al.*, "A data acquisition system for coincidence imaging using a conventional dual head gamma camera", *IEEE Nucl. Sci Symposium 7 Med. Img. Conference*, Nov. 9-15, Albuquerque, NM, USA, 1997
12. T. Kume, *et al.*, "Uptake and transport of positron-emitting tracer(18F) in plants", *Applied Radiation and Isotopes*, **48**, 1035-1043,1997.
13. D.J. Parker, *et al.*, "Industrial positron-based imaging: principles and applications", *Nucl. Instr. and Meth. A*, **348**, 583-592, 1994.
14. G. M. Field, *et al.*, "Mechanics of powder mixing using positron emission tomography", *Nucl. Instr. and Meth. A*, **310**, 435-436, 1991.